On-Line Detector Connectivity Check Based on a Parasitic Signal Coupling

Csaba F. Hajdu*†, Tamás Dabóczi†, Christos Zamantzas*
*European Organization for Nuclear Research (CERN), Geneva, Switzerland. Email: {cshajdu,czam}@cern.ch
†Budapest University of Technology and Economics, Department of Measurement and Information Systems, Budapest, Hungary. Email: {chajdu,daboczi}@mit.bme.hu

***Abstract*—Beam loss monitoring (BLM) is a key element of the scheme for machine protection and beam setup at the European Organisation for Nuclear Research (CERN). The project related to this paper aims to elaborate a process ensuring a comprehensive and continuous surveillance of the entire BLM signal chain, particularly the functionality and connectivity of the detectors. This paper presents a method elaborated with the view to realizing a noninvasive detector connectivity check.**

I. Introduction

The European Organisation for Nuclear Research (CERN) is one of the world's leading particle physics research laboratories, hosting a complex of particle accelerators dedicated to fundamental research. The particles injected into the flagship machine of the complex, the Large Hadron Collider (LHC), are first accelerated to progressively increasing energies through a series of preaccelerators known as the LHC injectors.

These aging low energy machines are being overhauled and consolidated within the framework of the LHC Injectors Upgrade (LIU) project in order to meet the more and more stringent requirements that the evolution of the LHC imposes on the quality of the particle beams.

The measurement of the showers of secondary particles generated by particles under acceleration escaping the beam lines is referred to as beam loss monitoring (BLM). The strategy for machine protection and beam setup at CERN relies heavily on BLM systems. A continuous supervision of the entire BLM signal and processing chain is therefore fundamental, yet no particle accelerator in the world has this feature at present.

This paper presents the latest results of a project aimed at designing a process providing such continuous surveillance for the new BLM system currently under development for the injectors, mandated by the LIU project.

II. Beam loss monitors

A. Beam loss monitoring at CERN in brief

The beam loss monitoring system of the LHC uses mainly ionization chambers as detectors. The ionizing particles crossing the gas-filled active volume of the chamber create electrons and ions, which are separated by a bias high voltage applied to the extremities of the detector and collected on a stack of parallel electrodes. The resulting current signal is acquired and digitized by the front-end cards of the system, then forwarded to the back-end electronics for further processing. The measured data are archived for machine tuning and calibration purposes, and if necessary for protecting the machines from damage caused by the beam, the safe extraction of circulating beams and an inhibition of further injections is initiated.

The new BLM system for the injectors is in an advanced stage of development at present. Currently, two prototypes of the system are installed: one in the laboratory, and one at the Proton Synchrotron Booster (PSB) accelerator alongside the operational system currently used for machine protection. Each front-end card of the BLM system for the injectors is capable of acquiring the output current of eight detectors [1]. The digitized signals are forwarded to the back-end card over a bidirectional optical link for further processing. These cards feature reprogrammable FPGA devices to ensure flexibility and high data throughput. The acquisition stage of the new system has been designed to be flexible and accommodate various detector types. In most locations, ionization chambers similar to those in the LHC system will be installed [2].

B. Connectivity checks

The current best solution for supervising the functioning of a beam loss monitoring system along with the correct connection and functionality of its detectors is in operation at the LHC, where a connectivity check of each detector channel is enforced every 24 hours. This procedure, only executable while the accelerator is offline, involves inducing a sinusoidal modulation on the order of $10\,\mathrm{mHz}$ in the bias high voltage of the ionization chambers, then measuring the resulting modulation in the output current of each channel. If the cabling connection of a detector is defective, the harmonic modulation will not be detectable in its output current. Additionally, correspondence has been found between variations in the amplitude and phase of the modulation in the output signal and various nonconformities of the acquisition chain, thus, this process is also usable as a component integrity survey.

The project related to this paper targets the elaboration of an improved procedure, to be constructed, tested and integrated into the BLM system of the injectors. The process should provide a continuous supervision of the entire signal chain from the detectors to the processing electronics as well as the measurement ability of the detectors.

Tamás Dabóczi acknowledges the support of ARTEMIS JU and the Hungarian National Research, Development and Innovation Fund in the frame of the R5-COP project.

III. The suggested measurement method

A. Approach for a non-invasive connectivity check

A series of measurements have been conducted on the prototype of the BLM system for the injectors to assess the capabilities of the signal processing chain [3], with a view to implementing a connectivity check process relying on modulating the high voltage supply of the detectors, similarly to the LHC implementation. This investigation has revealed that parasitic components corresponding to the switching frequency of about 30 kHz of the high voltage power supply (HVPS) and its harmonics are consistently present in the digitized output signal of the detectors. The detection of these parasitic components is very appealing, since it may allow verifying detector connectivity continuously by simply post-processing the digital signal without altering the analog signal in any way, thereby realizing a non-invasive on-line connectivity check. Further studies will be required for assessing how these components are coupled into the signal chain and which connection nonconformities can be detected by this approach. The part of the work described in the present paper is aimed at detecting this parasitic signal efficiently within the hardware constraints imposed by the architecture of the BLM system.

The resonator-based spectral observer (Fourier analyzer, FA) proposed by Péceli [4] was chosen as basis for a signal processing method to detect the spectral peaks resulting from the operation of the HVPS. Its advantages include inherent stability due to the unit negative feedback in the observer, flexibility in setting the frequencies of the observer channels [5], and that a straightforward frequency adaptation method [6] has been suggested for it, which should allow tracking the slowly varying frequency of the HVPS components.

B. The adaptive Fourier analyzer

One obtains the Fourier analyzer when using Péceli's resonator-based observer as a spectral observer. The structure estimates the state variables of the conceptual signal model [4], which can in turn be interpreted as a multisine generator reconstructing the signal from its DFT. In this interpretation, the state variables of the observer correspond to the complex Fourier coefficients of the signal and they each represent a harmonic resonator of the corresponding frequency.

The state variables, i.e. the complex Fourier components of the signal y_n can then be estimated using an appropriately designed observer, of the structure shown in Fig. 1, described by the following system equations:

$$\hat{\mathbf{x}}_{n+1} = \hat{\mathbf{x}}_n + \mathbf{g}e_n = \hat{\mathbf{x}}_n + \mathbf{g}\left(y_n - \hat{y}_n\right), \tag{1}$$

$$\hat{\mathbf{x}}_n = \left[\hat{x}_{i,n}\right]^T \in \mathbb{C}^{N\times 1}, \qquad i = -K, \ldots, K, \tag{2}$$

$$\hat{y}_n = \mathbf{c}_n^T \hat{\mathbf{x}}_n, \tag{3}$$

$$z_i = e^{j2\pi i f_0}, \tag{4}$$

$$\mathbf{c}_n = \left[c_{i,n}\right]^T \in \mathbb{C}^{N\times 1}, \qquad c_{i,n} = e^{j2\pi i f_0 n} = z_i^n, \tag{5}$$

$$\mathbf{g}_n = \left[g_{i,n}\right]^T \in \mathbb{C}^{N\times 1}, \qquad g_{i,n} = \frac{\alpha}{N} c_{i,n}^*, \tag{6}$$

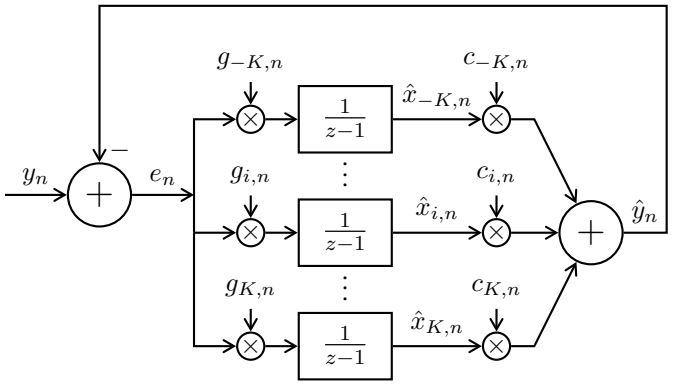

Figure 1. Block diagram of the resonator-based observer.

where $\hat{x}_{i,n}$ are the estimators of the state variables, thus of the complex Fourier components of the signal, $\hat{y}_n$ is the estimated signal and e_n is the estimation error. The vector $\mathbf{c}_n$ is the time-varying coupling vector to calculate the estimator of the signal from the state variables, while $\mathbf{g}_n$ represents the observer gain, a tunable parameter for setting the poles of the observer. The signal is considered to have K harmonics, thus $N = 2K + 1$ complex Fourier components including DC. For a real valued signal, the estimators of these components will form complex conjugate pairs: $\hat{x}_{i,n} = \hat{x}^*_{-i,n}$. The frequency of the fundamental harmonic relative to the sampling frequency is $f_0 = f_1/f_s$. It is assumed that $K \cdot f_1 \leq f_s/2$. If they're equal, $i = -K, \ldots, K+1$ and $N = 2K+2$ in all equations.

At this point, suppose that the frequency of the fundamental signal harmonic f_0 and the frequency of the fundamental resonator f_r, both expressed relative to the sampling frequency, are different. Then, the complex number estimating the Fourier coefficient of the fundamental harmonic is going to rotate with a frequency corresponding to the difference between f_0 and f_r [6], that is,

$$f_0 - f_r \approx \frac{\arg \hat{x}_{1,n+1} - \arg \hat{x}_{1,n}}{2\pi}, \tag{7}$$

which constitutes the basic principle of the methods for adapting f_r.

C. Realizing a customized spectral observer

As mentioned in Section II-A, front-end and back-end processing of the digitized data in the BLM system of the injectors is based on reconfigurable FPGA devices. This implies that ideally, data processing for on-line detector connectivity checks is realized on these FPGAs.

It's clear from (1)–(6) that the state update of the observer requires multiplications and additions of complex numbers. The polar representation ($z = Ae^{\mathrm{j}\varphi}$) would be convenient for multiplications, however, additions would require converting the numbers to the algebraic form ($z = a + \mathrm{j}b$), which is extremely resource-consuming on an FPGA. In the algebraic form, complex multiplications can be realized by a series of multiplications and additions, thus using this representation is preferable in terms of FPGA resource cost.

The digitized current values are represented using 20-bit integer arithmetic. For the FPGA implementation, we decided to use IEEE-754 compliant 32-bit floating point arithmetic realized with manufacturer-supplied IP cores to cope with the dynamic range expected from the inputs and the coefficients used for the state update.

For implementing the observer, we didn't rely on the linear time-variant (LTV) model presented in Section III-B. The observer model we chose is linear time-invariant (LTI) since it uses time-invariant $\mathbf{g}_n$ and $\mathbf{c}_n$ coefficients, but it's equivalent to the LTV model. It has the advantage that exponentiation of z_i as in (5) is not required. The problem with this calculation is that it is numerically unstable when using the algebraic form with 32-bit IEEE-754 arithmetic for certain values of $c_{i,1}$: $\lim_{n\to\infty} c_{i,n} = 0$ or ∞.

Our current implementation includes two parallel processing channels calculating the real and imaginary parts of the updated state variable separately. With a multiplier, an accumulator and a memory block storing the LTI coefficients, using the pipelining features of the floating point cores, each channel is capable of producing a new value every three clock cycles once the pipeline is full. The updated values for each state variable are calculated sequentially. This processing could be carried out in parallel for each resonator, and if necessary, all operations can be performed using just a single channel, which affords a big margin for tuning FPGA resource use versus processing speed.

The original observer structure was tailored heavily for an FPGA-based implementation. Since the output current of the detectors is acquired at a frequency of $500\,\mathrm{kHz}$ in the BLM system of the injectors, and the aim is to acquire a signal of about $30\,\mathrm{kHz}$ and its harmonics, the sampling frequency cannot be reduced by much. The observer runs at $500\,\mathrm{kHz}$ to ensure on-line data processing. Using sensible DFT bin widths of about $10 - 100\,\mathrm{Hz}$, this would yield an unmanageable number of resonators, since either the FPGA resource usage or the time required for processing would be too high. Thus, we considered an extremely coarse resonator distribution with the DFT points placed at the HVPS frequency and its harmonics. If slower convergence can be tolerated, the bandwidth of the resonator channels may be controlled by tuning the $\frac{\alpha}{N}$ parameter. This allows achieving an acceptable frequency sensitivity as shown in Fig. 2, without impacting on the stability of the structure.

In order to have an estimate of the noise floor in the measurement along with the value of the signal component of interest, we turned some of the individual resonators at lower frequencies into resonator triplets by adding two resonator positions on either side of the resonator in question. However, if the observer gain $\frac{\alpha}{N}$ is set so high that the bandwidths of neighboring resonators overlap, resonances may occur.

D. The new method for frequency adaptation

1) Principle: Using (7) directly for frequency adaptation would require calculating the phases of complex numbers, which is a resource-consuming task better avoided. Moreover,

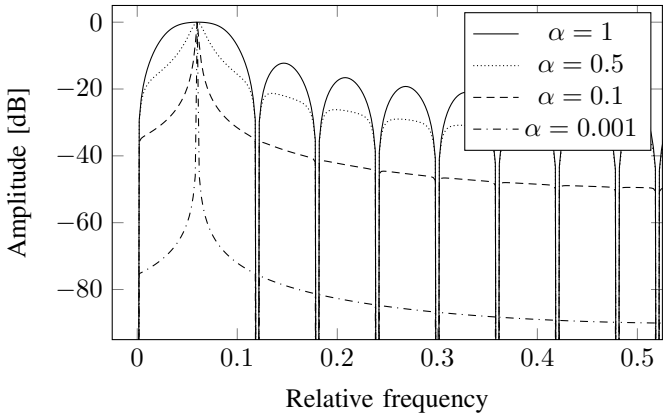

Figure 2. Transfer function of a resonator channel for different values of α. Its center frequency is $f_{rel} = 0.06$, that is, $30\,\mathrm{kHz}$ at $f_s = 500\,\mathrm{kHz}$. The transfer function has zeroes at the frequencies of the other resonators.

the phase of the Fourier coefficients tends to have abrupt transients when processing the output current of the detectors, which might misguide the adaptation. Therefore, we devised a method to adapt the frequency without having to calculate actual phases: we detect zero crossings in phase. This is very simple when using the algebraic form, since one only needs to consider the sign bits of the real and imaginary parts of the complex number. We need to make sure we exclude those events when the phase wraps from π to $-\pi$ or vice versa, since technically, the phase crosses zero even in these cases. Taking this consideration into account, we register an event if $\mathrm{Im}\{\mathrm{x}_{1,\mathrm{n}}\}$ changes sign while $\mathrm{Re}\{\mathrm{x}_{1,\mathrm{n}}\} \geq 0$. Then, if N_z zero crossings have been registered in a time window of t_m, we have the following estimate for the frequency difference:

$$|f_0 - f_r| \approx \frac{(N_z - 1)\cdot 2\pi}{t_m \cdot f_s}\,\frac{1}{2\pi} = \frac{N_z - 1}{t_m \cdot f_s}, \qquad (8)$$

where the sign of the difference can be determined by considering the *sign* of the zero crossing: if $\mathrm{Im}\{\mathrm{x}_{1,\mathrm{n}}\}$ changes from negative to positive, we register a positive zero crossing corresponding to $f_0 > f_r$, and the opposite for negative zero crossings. At the expense of slower adaptation, this scheme can be implemented at a comparatively low cost in terms of FPGA resources and it's also less subject to the effect of abrupt transients in the phase signal.

2) Implementation: The source of the parasitic signal we're aiming to detect is the same HVPS for all eight channels of the same card, thus we decided to carry out frequency adaptation on one channel only and use the same coefficient values for all channels.

The frequency adaptation principle described in Section III-B relies on the LTV model of the observer. Our realization calculates LTI state variables, which thus need to be multiplied by z_i^n for conversion to LTV. This exponentiation is subject to the numerical problems described in Section III-C. Since z_i is recalculated every time the frequency is adapted, this effect is mitigated but not eliminated.

If the input signal is noisy, repetitive fake zero crossing events like those shown in Fig. 3 may occur. These can be eliminated by setting an adequate minimum time difference requirement between consecutive zero crossings and ignoring those violating this constraint.

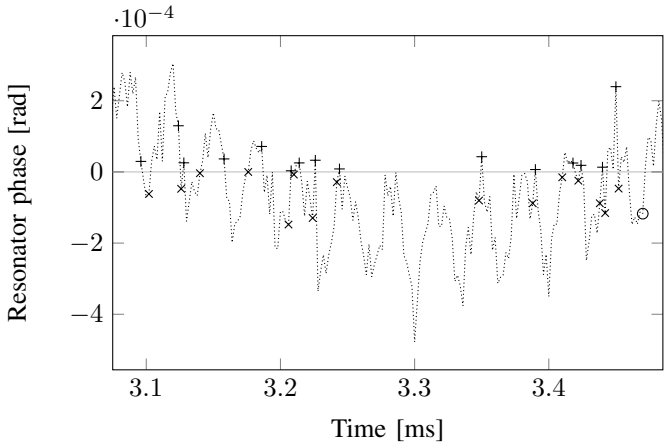

Figure 3. Spurious zero crossings caused by noise in the phase of $\hat{x}_{1,n}$ calculated from a real signal acquisition. The markers × and + correspond to rejected positive and negative zero crossings, respectively, while ○ represents the one accepted positive zero crossing.

Additionally, transients in phase resulting from noise may cause the processing to register alternating positive and negative zero crossings. In our scheme, we count these events separately, either until a given number of events of either type is collected or for a given amount of time, and then we use the difference $N_{z+} - N_{z-}$ to calculate the estimate of the frequency difference. Currently, we acquire 128 events of either type, adapt the frequency, then discard the first 128 events to suppress the transients caused by the adaptation.

Since calculating the new set of coefficients using FPGA logic directly would imply prohibitively high resource usage, we decided to carry out this processing on a very simple soft-core CPU embedded in the FPGA. Since the CPU features no floating-point core, all floating-point arithmetic is executed in software, therefore calculating a new set of coefficients for the 13 resonators we currently use takes about $0.1\,\mathrm{s}$. Since the adaptation itself is fairly slow, this time overhead is acceptable.

E. Results with the custom adaptive observer

We tested the current version of our processing with frequency adaptation both in the laboratory system and the prototype installed at the PSB.

The performance of the frequency adaptation in the laboratory system is demonstrated in Fig. 4. The processing is capable of following the slow frequency drift satisfactorily.

As a tradeoff between limiting the noise in the signal and ensuring the detectability of the HVPS contributions, our resonators have a bandwidth of about $5-10\,\mathrm{Hz}$. The resonator outputs react to beam loss events, but the recovery is fairly quick (about $0.1-0.5\,\mathrm{s}$) and these contributions can be filtered out. They also have little effect on frequency adaptation. In general, the resonators centered on the HVPS peak show values about $20\,\mathrm{dB}$ higher than the other resonators of the triplet if the HVPS contributions are present.

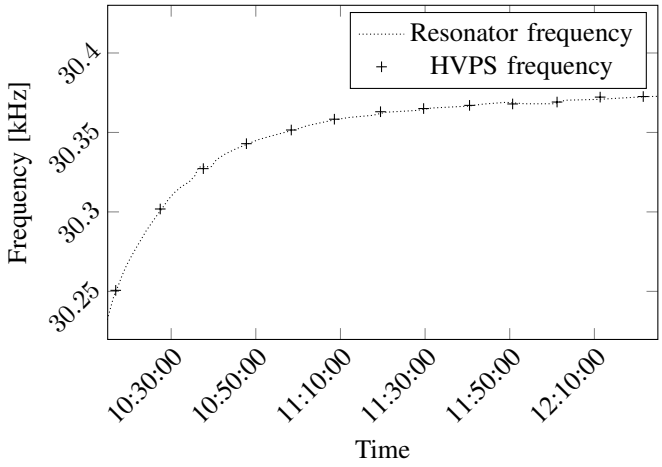

Figure 4. Demonstration of frequency tracking by the resonator-based observer: evolution of the fundamental resonator frequency, registered at each frequency adaptation step. The variation of the fundamental frequency of the HVPS contributions is also shown: every marker (+) represents an acquisition.

Under real operating conditions, our method usually seems to underestimate the actual frequency difference, especially if it is relatively high. However, we've seen the frequency adaptation converge for initial differences as high as $500\,\mathrm{Hz}$. In our experience, this covers the frequency band the HVPS signal fluctuates in.

IV. Conclusions

We presented a method to identify parasitic components caused by the operation of the high voltage power supply in the output current of the BLM detectors. Further studies will need to be conducted to determine precisely how this signal is coupled into the signal chain and which connection nonconformities can be detected by this approach. An extension of the procedure to cover all faults targeted by the LHC implementation is foreseen.

References

[1] W. Viganò, M. Alsdorf, B. Dehning, M. Kwiatkowski, G. G. Venturini, and C. Zamantzas, "10 Orders of Magnitude Current Measurement Digitisers for the CERN Beam Loss Systems," *J. Instrum.*, vol. 9, p. C02011. 10 p, Sep 2013.

[2] C. Zamantzas, M. Alsdorf, B. Dehning, S. Jackson, M. Kwiatkowski, and W. Viganò, "System Architecture for measuring and monitoring Beam Losses in the Injector Complex at CERN," Tech. Rep. CERN-ACC-2013-0252, CERN, Geneva, Aug 2012.

[3] C. F. Hajdu, T. Dabóczi, and C. Zamantzas, "Design and implementation of a real-time system survey for beam loss monitoring systems," in *XXI IMEKO World Congress - Full Papers*, pp. 1176–1180, 2015.

[4] G. Péceli, "A common structure for recursive discrete transforms," *Circuits and Systems, IEEE Transactions on*, vol. 33, pp. 1035–1036, Oct 1986.

[5] G. Péceli, "Sensitivity properties of resonator-based digital filters," *Circuits and Systems, IEEE Transactions on*, vol. 35, no. 9, pp. 1195–1197, 1988.

[6] F. Nagy, "Measurement of signal parameters using nonlinear observers," *Instrumentation and Measurement, IEEE Transactions on*, vol. 41, pp. 152–155, Feb 1992.